Zeolites

DOI: 10.1002/anie.201105738

Assemblies of Mesoporous FAU-Type Zeolite Nanosheets**

*Alexandra Inayat, Isabel Knoke, Erdmann Spiecker, and Wilhelm Schwieger**

Hierarchical porous materials are of great scientific as well as technological interest because the presence of porosity on different scales has the potential to affect the transport characteristics of molecules within the pore system. The targeted design of the pore hierarchy in such materials will result in improved performance in transport-based applications, such as adsorption, catalysis, and separation.[1,2]

Hierarchical materials containing zeolites, combine characteristics of systems with pore sizes on at least two different length scales.[3,4] Compared to the allover microporous channels in conventional zeolite crystals, such hierarchical pore systems, with wide transport pores intersecting the micropore network like motorways linking a narrow road system, are already proven to reduce diffusion limitations for molecules within zeolitic catalysts.[5–10] While for high-silica zeolites, such as ZSM-5, several methods for incorporating additional transport pores were developed during the past few years,[3,4,11] such a substantial collection of approaches is not available for low-silica zeolites. Herein, we present the synthesis and characterization results of Faujasite (FAU)-type zeolite X ($Si/Al < 1.5$) grown as house-of-cards-like nanosheet assemblies with intracrystalline mesoporosity. The resulting pore system covers all three pore size levels (micro-meso-macro) in a hierarchical interconnection.

The reduction of diffusion limitations in microporous zeolites can be achieved by the creation of intracrystalline transport pores (in the meso or macro pore range) or by the reduction of the zeolite crystal dimensions itself.[11] Zeolite crystals with additional meso (or in few cases macro)[12] pores can be produced by different methods,[13] for example, desilication by an alkaline post-treatment[14,15] or by the use of hard[16,17] and soft[9,18–20] templates during zeolite synthesis.

However, all the methods are usually limited to a certain group of zeolites or just to a special zeolite type. For example, for zeolites with a Si/Al molar ratio below about 15, desilication is not an appropriate method for the introduction of additional transport pores.[8] Thus, it is very challenging to introduce transport pores into low-silica (high aluminum content) zeolites. To date, only the low-silica zeolites LTA and SOD could be synthesized with intracrystalline mesoporosity by soft-templating with organosilane surfactants such as 3-(trimethoxysilyl)propyl hexadecyl dimethyl ammonium chloride (TPHAC).[19,20] There are a few reports on the synthesis of mesoporous FAU-type zeolite Y, either by using carbon aerogel as a hard template,[17] by steaming,[21] or by a combined acid–base post-treatment.[22] With the acid–base technique a threefold hierarchical pore system, combining the zeolitic micropores and two ranges of mesopores, was obtained with a resulting Si/Al molar ratio of around 20. But owing to the underlying extraction mechanism, this combined acid–base post-treatment is (as well as the single alkaline post-treatment) not suitable for introducing mesopores into low-silica zeolites with Si/Al molar ratios close to 1.

Furthermore, all the examples reported for hierarchical zeolites involve either a micro/meso[12,16,17,19–22] or a micro/macro[12] pore size combination, but to our knowledge there is no zeolitic material which combines pores of all three (micro-meso-macro) size levels hierarchically interconnected within one particle.

In fact, for Faujasite-type zeolite X, a highly hydrophilic large-pore zeolite with a pore diameter of about 0.74 nm and with a low Si/Al molar ratio of 1.0–1.5, a successful method for the creation of additional transport porosity has not been reported up to now. This limitation is a drawback, especially from the viewpoint of using renewable feedstocks for the production of so-called new platform chemicals. Such processes usually involve the transformation of larger molecules, such as fatty acids or sugars. In this area especially basic catalysts such as zeolite X[23] are of high importance, for example for transesterification reactions.[24,25] Thus it seems to be an essential task to design the properties of such catalysts according to the future demands. Consequently, our major aim was to find a facile synthesis pathway for the implementation of additional transport porosity in Faujasite-type zeolite X.

For the synthesis of the mesoporous zeolite X nanosheets the organosilane template TPHAC was used. The as-synthesized material was designated NaX-T, and after template removal by calcination as NaX-T-cal. For comparison purpose a conventional microporous zeolite X (NaX-R, NaX-R-cal) was synthesized using the same synthesis conditions and composition but without TPHAC. As can be seen from the powder X-ray diffraction (XRD) patterns in Figure 1, the reflections of both synthesis products could be attributed to the Faujasite structure and were indexed accordingly.[26]

Competing crystalline phases such as zeolite LTA and zeolite P (GIS structure) were not observed. Furthermore, the absence of a halo between $2\theta = 25$–$30°$ in the XRD patterns as well as the absence of sponge-like material in the SEM pictures in Figure 2 indicate the absence of amorphous material. Elemental analysis gave a Si/Al molar ratio of 1.2

[*] A. Inayat, Prof. W. Schwieger
Chair of Chemical Reaction Engineering, Department of Chemical and Bioengineering, University of Erlangen-Nuremberg
Egerlandstrasse 3, 91052 Erlangen (Germany)
E-mail: wilhelm.schwieger@crt.cbi.uni-erlangen.de
Dr. I. Knoke, Prof. E. Spiecker
Center of Nanoanalysis and Electron Microscopy (CENEM), Department of Material Sciences, University of Erlangen-Nuremberg, Cauerstrasse 6, 91058 Erlangen (Germany)

[**] We gratefully acknowledge funding by the Fonds der Chemischen Industrie (FCI) and by the German Research Council (DFG), which supports the Cluster of Excellence "Engineering of Advanced Materials" at the University of Erlangen-Nuremberg.

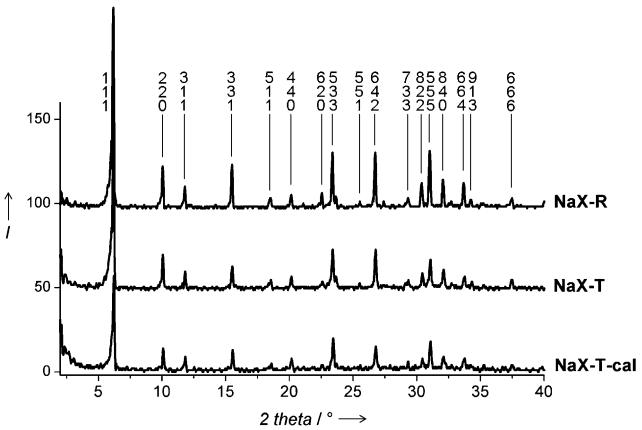

Figure 1. X-ray diffraction patterns of the reference zeolite X sample (NaX-R) and the nanosheet sample, as-synthesized (NaX-T) and calcined (NaX-T-cal).

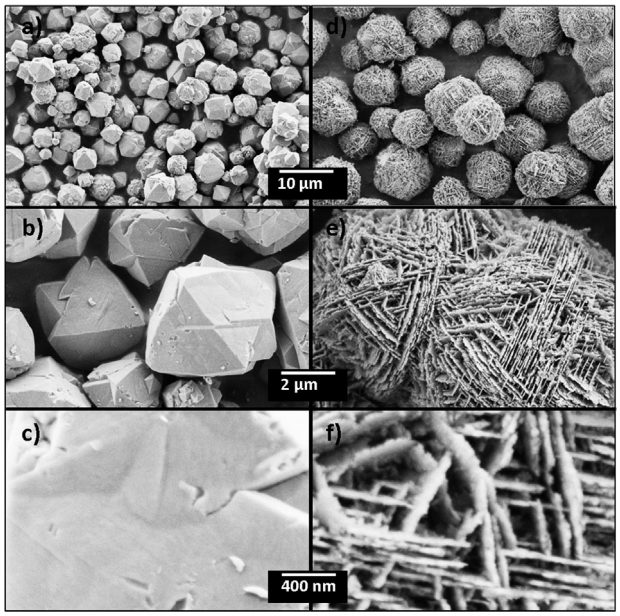

Figure 2. SEM pictures with different magnifications of a–c) calcined conventional (reference) zeolite X (NaX-R-cal) and d–f) hierarchical zeolite X (NaX-T-cal).

for both NaX-R-cal and NaX-T-cal, which is in the expected range of 1.0–1.5 for Faujasite-type zeolite X.

The SEM images in Figure 2 show a morphological comparison between the conventional zeolite X crystals (NaX-R-cal) and the zeolite X sample synthesized in the presence of TPHAC (NaX-T-cal). NaX-R-cal crystals have a compact octahedral shape which is typical for zeolite X.[27] In contrast, NaX-T-cal consists of ball-shaped house-of-cards-like nanosheet assemblies. These nanosheet balls have a larger diameter (ca. 9 µm) than the conventional zeolite X crystals (ca. 4 µm), but the triangular form of the crystal faces is still recognizable in the triangular arrangement of the zeolitic nanosheets (see Figures 2 b,e).

Note that the formation of zeolitic nanosheets induced by the use of TPHAC has not been observed with any other zeolite type.[18–20] In these other cases the presence of TPHAC led to the formation of quite compact zeolite crystals (SOD, MFI, or LTA) with intracrystalline mesoporosity.[18–20] Nanosheet assemblies similar to those observed herein for zeolite X (Figure 2) but without intracrystalline mesoporosity were only reported for MFI-type zeolite syntheses using the diquaternary ammonium-type surfactant $C_{22}H_{45}$-$N^+(CH_3)_2$-C_6H_{12}-$N^+(CH_3)_2$-C_6H_{13}.[9] The reason for this different behavior in the case of zeolite X might be an interplay between the surface activity of the $TPHA^+$ molecules and the charge-balancing effects of the inorganic cations in the given synthesis composition, which respectively, lead to the formation of micellar assemblies and direct the zeolite crystallization into a twinned crystal growth. Such twinning is known from various crystal types, for example, gismondine (zeolite P).[28]

Nitrogen physisorption isotherms and pore size distribution curves of the calcined nanosheet assemblies (NaX-T-cal) and of the reference zeolite X sample (NaX-R-cal) are depicted in Figure 3.

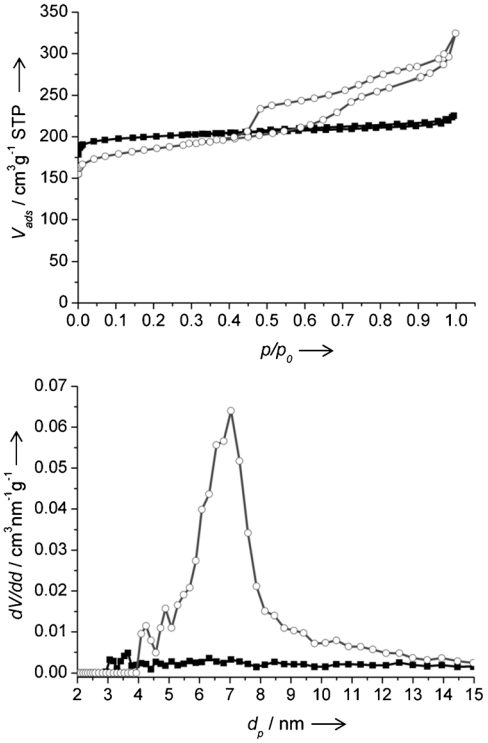

Figure 3. Nitrogen physisorption isotherm (top) and derived pore size distribution curves (bottom) of conventional zeolite X (NaX-R-cal, ■) and the nanosheet assemblies (NaX-T-cal, ○).

As expected, the calcined reference zeolite X sample (NaX-R-cal) shows a type I isotherm according to the IUPAC classification, typical for completely microporous materials. In contrast, the isotherm of the calcined zeolite X nanosheets (NaX-T-cal) shows a significant increase of the adsorption branch between 0.4 and 0.8 p/p_0 and a pronounced hysteresis

loop. This type IV isotherm is typical for mesoporous materials. Accordingly, the pore size distribution curve of the zeolitic nanosheets exhibits mesopores with a most frequent pore diameter of around 7 nm. The texture data of both samples are summarized in Table 1. It can be seen that

Table 1: Texture data (pore volume V, specific surface area S, most frequent mesopore diameter d_p) from nitrogen physisorption.

Sample	V_{micro} [$cm^3 g^{-1}$]	V_{meso} [$cm^3 g^{-1}$]	V_{total} [$cm^3 g^{-1}$]	S_{BET}/S_{DR} [$m^2 g^{-1}$]	S_{ext} [$m^2 g^{-1}$]	d_p [nm]
NaX-R-cal	0.32	0.04	0.36	812/853	11	–
NaX-T-cal	0.26	0.20	0.50	724/763	130	7.0

the calculated micropore volume of the mesoporous nanosheets is lower than that of the compact zeolite X crystals (NaX-R-cal) whereas their external surface area S_{ext}, mesopore, and total pore volume are much higher, which is in agreement with the observations made by other authors after the introduction of mesoporosity into microporous zeolites.[8,29]

To specify the location of the mesopores in the calcined nanosheets (NaX-T-cal), this sample was investigated by means of transmission electron microscopy (TEM). In Figure 4, images of the samples NaX-T-cal (Figure 4a–c) and NaX-R-cal (Figure 4d–f) are shown. Special care was taken to keep the electron dose low to avoid amorphization of the samples.

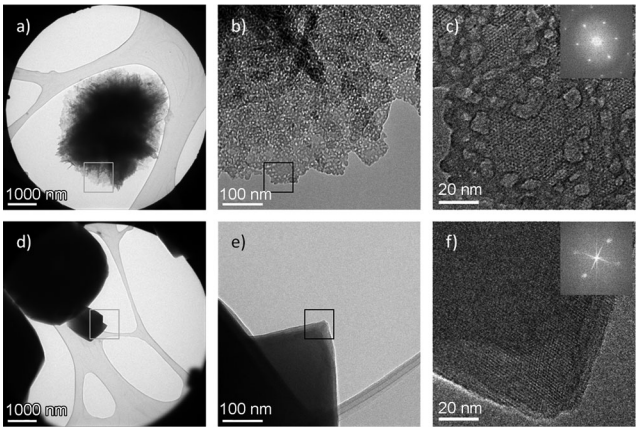

Figure 4. TEM images of the mesoporous zeolite X nanosheets (NaX-T-cal, top row a–c) and of the conventional non-mesoporous zeolite X (NaX-R-cal, bottom row d–f): a) overview, b) enlarged area of a nanosheet showing mesopores, c) high-resolution image with Fast Fourier Transform (FFT) inset ([111] zone axis), d) overview, e) enlarged area, f) high-resolution image with FFT as inset ([110] zone axis). Squares in one image show the area enlarged in the next image.

The overview images Figure 4a and 4d confirm the morphology of the zeolites as seen by SEM (Figure 2). NaX-T-cal shows mesopores in the nanosheets (Figure 4b). The image has been taken with objective aperture and a slight underfocus to enhance the bright contrast of the mesopores. The mesopores show a rather narrow size distribution with pore diameters of about 8 nm which is in good agreement with the nitrogen physisorption results of approximately 7 nm (Figure 3, bottom). The arrangement of the mesopores in the nanosheets can be seen from the high-resolution image Figure 4c taken in [111] zone axis. This image also shows the hexagonal array of the zeolitic micropores. Hence, it can be concluded that the zeolitic nanosheets contain intracrystalline mesopores. The TEM images of the conventional zeolite X sample NaX-R-cal (Figure 4e,f) were taken to ensure that the observed mesoporosity in the nanosheets was not caused by the electron beam during measurement. Comparison of the high-resolution image Figure 4f taken in the [110] zone axis with that of sample NaX-T-cal (Figure 4c) confirms that both samples have the same crystal structure, but that the conventional zeolite X (NaX-R-cal) does not have any mesopores.

In summary, it was shown that Faujasite-type zeolite X crystals can be synthesized with a unique, threefold hierarchical pore system. This pore system is constructed of zeolitic nanosheets in a house-of-cards-like assembly with wide macroporous interstices between the nanosheet stacks. Within each nanosheet there are intracrystalline mesopores with diameters of around 7 nm from which the zeolitic micropores (0.74 nm wide pore openings) can be accessed (Figure 5). This hierarchical pore arrangement connects the zeolitic micropores through the mesopores and macroporous channels (interstices between the nanosheets) with the outside medium. The accessibility of the micropores and the zeolite surface from and to the outside (see arrows (a) and (b) in Figure 5) has been greatly improved. Thus, this new zeolitic material might have great potential for use as an adsorbent or

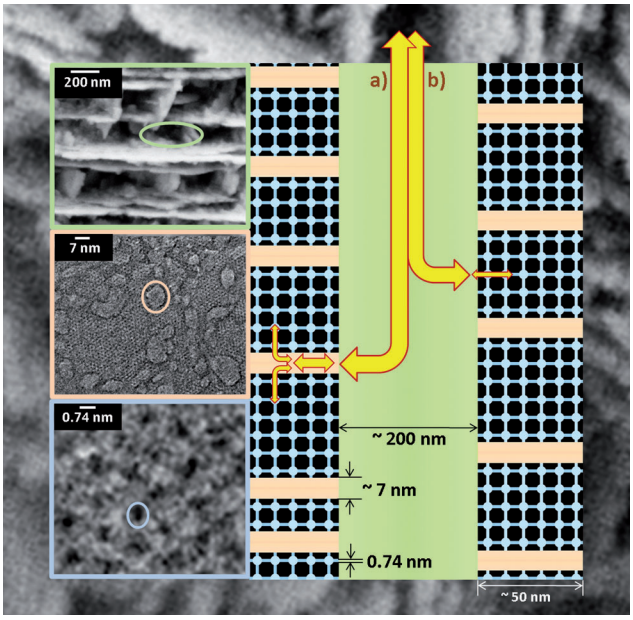

Figure 5. Schematic representation of the three different hierarchy levels in the pore structure of the mesoporous zeolite X nanosheet sample (NaX-T-cal), 200 nm = macropores; 7 nm = mesopores; 0.74 nm = micropores; arrows on the right hand side: possible flow paths within the hierarchical pore system: route a) macro-meso-micro, route b) macro-micro.

a catalyst in processes involving diffusion-limited steps for a wide variety of larger molecules.

Experimental Section

For the synthesis of zeolite X sodium silicate solution (mass%: 26.5 SiO_2, 8.3 Na_2O, 65.2 H_2O, Merck), NaOH (97%, Merck) and distilled water were mixed at room temperature before sodium aluminate solution (mass%: 19.1 Al_2O_3, 19.8 Na_2O, 61.1 H_2O, Süd-Chemie AG) was added under vigorous stirring. After the mixture was stirred for 1 h at 1300 rpm, TPHAC (50 mass% methanolic solution, synthesized according to Ref. [30]) was added. The obtained gel with molar composition 1 Al_2O_3 : 3.5 Na_2O : 3 SiO_2 : 180 H_2O : 0.06 TPHAC was aged for 1 day at room temperature and statically crystallized in polypropylene bottles at 75 °C for 4 days in a convection oven. Afterwards the product was isolated by vacuum filtration, washed with distilled water until pH 8 and dried at 75 °C (sample denoted as NaX-T). The organic template was removed by calcination in a muffle furnace at 650 °C in 80 mL min^{-1} air flow with a heating ramp of 2 K min^{-1} and an isothermal step of 8 h. White powders were obtained (NaX-T-cal). A reference sample (NaX-R, NaX-R-cal) was produced in the same way as described above, but without TPHAC.

Powder XRD patterns were recorded in a Philips X′pert Pro diffractometer operated at 40 kV and 40 mA using CuK_α radiation in steps of 0.02° with a sampling time of 1 s per step.

SEM pictures were recorded with the electron microscope ULTRA55 (Carl Zeiss MST AG). TEM measurements were performed with a Phillips CM300-UT transmission electron microscope operating at an acceleration voltage of 300 kV. Samples were dispersed with isopropanol on a lacey carbon film and dried over night at 110 °C.

Nitrogen physisorption was conducted at 77 K in a Quantachrome Quadrasorb SI instrument. Prior to the measurements the samples were outgassed for 12 h at 300 °C under vacuum. Pore size distribution curves were calculated from the adsorption branch of the isotherm according to the Quantachrome DFT kernel for nitrogen at 77 K in cylindrical silica pores. Micropore volumes were determined as the DFT cumulative pore volume for pores below 2 nm pore diameter. The mesopore volume was obtained as the DFT cumulative pore volume for pores between 2 and 50 nm pore diameter. The total pore volume was calculated from the adsorption point at 0.99 p/p_0. Specific surface areas were obtained from the Brunauer–Emmet–Teller (BET) equation in the linear range between 0.01 and 0.20 p/p_0 and from the Dubinin–Radushkewich (DR) method. The external surface area is regarded as the difference between total surface area (S_{BET}) and micropore surface area and was calculated using the t-plot method (t-plot in the linear statistical thickness range between 0.5 and 0.7 nm).

For elemental analysis inductively coupled plasma optical emission spectroscopy (ICP-OES, instrument Plasma 400, PerkinElmer, USA) was used.

Received: August 13, 2011
Revised: November 29, 2011
Published online: January 16, 2012

Keywords: hierarchy · mesoporous materials · nanosheets · soft templating · zeolites

[1] G. Wang, E. Johannessen, C. R. Kleijn, S. W. de Leeuw, M.-O. Coppens, *Chem. Eng. Sci.* **2007**, *62*, 5110.
[2] D. Zhao, P. Yang, B. F. Schmelka, G. D. Stucky, *Chem. Mater.* **1999**, *11*, 1174, and references therein.
[3] S. Lopez-Orozco, A. Inayat, A. Schwab, T. Selvam, W. Schwieger, *Adv. Mater.* **2011**, *23*, 2602.
[4] Z. L. Hua, J. Zhou, J. L. Shi, *Chem. Commun.* **2011**, *47*, 10536.
[5] R. Valiullin, J. Kärger, K. Cho, M. Choi, R. Ryoo, *Microporous Mesoporous Mater.* **2011**, *142*, 236.
[6] R. Valiullin, J. Kärger, *Chem. Ing. Tech.* **2011**, *83*, 166.
[7] C. H. Christensen, K. Johannsen, E. Törnqvist, I. Schmidt, H. Topsøe, C. H. Christensen, *Catal. Today* **2007**, *128*, 117.
[8] J. Pérez-Ramírez, C. H. Christensen, K. Egeblad, C. H. Christensen, J. C. Groen, *Chem. Soc. Rev.* **2008**, *37*, 2530.
[9] M. Choi, K. Na, J. Kim, Y. Sakamoto, O. Terasaki, R. Ryoo, *Nature* **2009**, *461*, 246.
[10] J. C. Groen, W. Zhu, S. Brouwer, S. J. Huynink, F. Kapteijn, J. A. Moulijn, J. Perez-Ramirez, *J. Am. Chem. Soc.* **2007**, *129*, 355.
[11] J. van den Bergh, J. Gascon, F. Kaptejn in *Zeolites and Catalysis—Synthesis Reactions and Applications*, *Vol. 1* (Eds.: J. Cejka, A. Corma, S. Zones), Wiley-VCH, Weinheim, **2010**, chap. 13.
[12] J. C. Groen, L. A. A. Peffer, J. A. Moulijn, J. Perez-Ramirez, *Chem. Eur. J.* **2005**, *11*, 4983.
[13] K. Egeblad, C. H. Christensen, M. Kustova, C. H. Christensen, *Chem. Mater.* **2008**, *20*, 946.
[14] D. Verboekend, J. Perez-Ramirez, *Chem. Eur. J.* **2011**, *17*, 1137.
[15] J. C. Groen, J. A. Moulijn, J. Perez-Ramirez, *J. Mater. Chem.* **2006**, *16*, 2121.
[16] C. J. H. Jacobsen, C. Madsen, J. Houzvicka, I. Schmidt, A. Carlsson, *J. Am. Chem. Soc.* **2000**, *122*, 7116.
[17] Y. Tao, H. Kanoh, K. Kaneko, *J. Phys. Chem. B* **2003**, *107*, 10974.
[18] M. Choi, H. S. Cho, R. Srivastava, C. Venkatesan, D.-H. Choi, R. Ryoo, *Nat. Mater.* **2006**, *5*, 718.
[19] K. Cho, H. S. Cho, L.-C. de Menorval, R. Ryoo, *Chem. Mater.* **2009**, *21*, 5664.
[20] V. G. Shanbhag, M. Choi, J. Kim, R. Ryoo, *J. Catal.* **2009**, *264*, 88.
[21] W. Lutz, D. Enke, W.-D. Einicke, D. Täschner, R. Kurzhals, *Z. Anorg. Allg. Chem.* **2010**, *636*, 2532–2534.
[22] K. P. de Jong, J. Zecevic, H. Friedrich, P. E. de Jongh, M. Bulut, S. van Donk, R. Kenmogne, A. Finiels, V. Hulea, F. Fajula, *Angew. Chem.* **2010**, *122*, 10272; *Angew. Chem. Int. Ed.* **2010**, *49*, 10074.
[23] R. J. Davis, *J. Catal.* **2003**, *216*, 396.
[24] O. Meyer, P. Adryan, J. Riedel, F. Roessner, R. A. Rakoczy, R. W. Fischer, *Chem. Ing. Tech.* **2010**, *8*, 82.
[25] S. Luz Martínez, R. Romero, J. C. López, A. Romero, V. Sánchez Mendieta, R. Natividad, *Ind. Eng. Chem. Res.* **2011**, *50*, 2665.
[26] M. M. J. Treacy, J. B. Higgins, *Collection of Simulated XRD Powder Patterns for Zeolites*, *5th ed.*, Elsevier, Amsterdam, **2007**, p. 170.
[27] N. S. John, S. M. Stevens, O. Terasaki, M. W. Anderson, *Chem. Eur. J.* **2010**, *16*, 2220.
[28] C. Baerlocher, W. M. Meier, *Z. Kristallogr.* **1972**, *135*, 339.
[29] Z. Yang, Y. Xia, R. Mokaya, *Adv. Mater.* **2004**, *16*, 727.
[30] K. J. Huettinger, M. F. Jung, *Chem. Ing. Tech.* **1989**, *61*, 258 and original manuscript *Chem. Ing. Tech.* MS 1742/89.

